Fermi National Accelerator Laboratory

TM-1631
[SSC-N-677]

Vacuum Technology Issues for the SSC*

Hans Jöstlein
Fermi National Accelerator Laboratory
P.O. Box 500, Batavia, Illinois 60510

October 23, 1989

* Talk presented at the Conference of the American Vacuum Society, Boston, Massachusetts, October 26, 1989. To be published in J. Vac. Sci. Tech.

Operated by Universities Research Association, Inc., under contract with the United States Department of Energy

Vacuum Technology Issues for the SSC, H. Jöstlein, Fermi National Accelerator Lab, Batavia, Ill. 60510

The Superconducting Super Collider, to be built in Texas, will provide an energy of 40 TeV from colliding proton beams. This energy is twenty times higher than currently available from the only other cryogenic collider, the Fermilab Tevatron, and will allow experiments that can lead to a better understanding of the fundamental properties of matter.

The energy scale and the size of the new machine pose intriguing challenges and opportunities for the its vacuum systems.

The discussion will include the effects of synchrotron radiation on cryogenic beam tubes, cold adsorption pumps for hydrogen, methods of leak checking large cryogenic systems, the development of cold beam valves, and radiation damage to components, especially electronics.

Description of the SSC

The Superconducting Super Collider, already named "Super Clyde" by the friendly people in Waxahatchie, Texas, has recently been made a construction project. Congress has allocated some 250 M$. The SSC consists of two 20 TeV proton accelerator/storage rings, stacked on top of one another, in an underground racetrack tunnel (Fig. 1) of 83 km circumference. The two proton beams, one in each ring, will slam into each other at up to 8 crossing points, creating up to ninety million interactions a second at each crossing point. Fig. 2 shows the secondary particles (about 100 on average) emerging from such a collision observed at the Tevatron collider at Fermilab near Chicago, currently providing the highest energy in the world, 1 TeV on 1 TeV. The computer picture shows reconstructed tracks in a magnetic fields, which deflects them from a straight line depending on their momentum.

Machines such as the Supercollider will open up new experimentation into the fundamental nature of matter. While particle physics has now, for the first time, a coherent theory (the "Standard Model") explaining (nearly) all the observations on particle properties and interactions, there are a few tantalizing contradictions and unexplained properties that, we hope, can be studied when interactions at thousand times higher rates and twenty times higher energy will become available on the SSC.

Now that construction has started, one can expect a thorough review of all design aspects, probably followed by many changes. Meanwhile the picture has not much evolved yet from the 1986 status of the SSDC Design Report[1], and my remarks will be based on that design.

SSC layout/ The Accelerator Complex

While the SSC main rings dwarf all other installations at the site by sheer size, there is actually the last link in a cascade of several accelerators.

---

[1] Conceptual Design of the Superconducting Super Collider, SSC-SR-2020, March 1986

As is customary in proton storage rings, the beams originate in a negative hydrogen ion source, followed by a static preaccelerator. An Rf quadrupole then feeds the beam into a 600 MeV Linac. As seen in Fig. 3, a rapid cycling Low Energy Booster(LEB) accelerates the beam to 8 GeV, a Medium Energy Booster goes to 100 GeV, and a cryogenic superconducting High Energy Booster (now thought to provide an energy of 2 TeV, rather than the 1 TeV listed in the design report) prepares the beams for injection into the storage rings, which will take about 15 minutes to accelerate them to the 20 TeV design energy.

I will not say much about the fairly conventional accelerator complex, except to mention that the LEB cycles at 10 Hz, fast enough to induce large currents into a conducting vacuum chamber, disrupting magnetic fields. Past rapid cycling synchrotrons have placed the whole magnet string inside the vacuum, sidestepping the problem. New materials have made it possible to consider insulating vacuum chambers, coated with a high resistivity layers to avoid electrostatic charge buildup. Such materials include carbon fiber composites, clad with thin aluminum foil, or possibly ceramics, if new manufacturing processes can be found to make them. The pipes are typically 100 mm in diameter and 4.5 m long, beyond current ceramic fabrication capabilities.

SSC Dipole, Quadrupole, Cell

The two main rings each consist of a string of cryogenic superconducting magnets for 94% of the circumference, the rest being a conventional UHV system at 10^{-10} Torr. The cold strings are each assembled from 664 repeating, 96m long "half cells", each containing five 17 m long dipole magnets, a 4m quadrupole and a 5m "drift" space for other devices.

Vacuum Spaces

The beam pipe is innermost and operates at a temperature of 4.5 K or even 1.8 K if supercooling is used. Its pressure will be well below 10^{-10} Torr due to the natural cryo pumping. The beam pipe will probably be a 40 mm diameter stainless steel tube with an 0.1 mm pure copper coating on the inside to conduct the high frequency beam image currents. More work is needed to identify the best and most economic way to produce the coating. The pipes will have to be baked and cleaned to UHV standards, and maintained free from dirt, oils, dust and fingerprints until each magnet gets installed and welded to its neighbor. This is a major logistics challenge!

The coil/cold iron yoke assembly and the surrounding liquid nitrogen shield (plus an intermediate 20K helium gas cooled shield) are wrapped in aluminized Mylar foil and placed in an outer vessel held at 10^{-6} Torr for thermal insulation(see Fig. 4). This pressure is also maintained by natural cryopumping.

Synchrotron Radiation Desorption

Process

The protons in the SSC move fast enough to emit synchrotron radiation. For comparison, the proton velocity, expressed by the relativistic gamma factor, is higher than that of the electrons in the 6 GeV synchrotron light source now under construction at Argonne. The SSC total radiated power is about 8 kW per ring, or 100 mW per meter of beam tube.

For room temperature beam tubes it is known that this light knocks gas atoms from the tube walls, leading to increased vacuum pressure. All new synchrotron light machines undergo a cleaning phase, where these gases are released and pumped away, until the desorption factor eta has dropped from an initial value near one neutral atoms released per each photon to values as low as 10^{-6} neutrals per photon.

The same desorption process was expected (and has been confirmed [2]) to occur in cold beam tubes, but additional desorption could also occur due to the low binding energy of adsorbants in cold tubes. The energy of a single photon is sufficient to release thousands of neutrals if a suitable mechanism exists. In fact, it has been shown many years ago that KeV-energy ions can each release thousands of neutrals from cold walls.

Measurements

To insure against any unknown "killer effects" in the SSC, an experimental study of cold desorption of neutrals by synchrotron radiation was carried out at the Brookhaven Light Source[3] and at KEK[4].

---

[2] D. Bintinger and P. Limon, J.Vac.Sci.Technol. A, Vol.7, No.1, Jan/Feb 1989

[3] D. Bintinger, "Notes on June 1987 PSD Runs at NSLS . . .", private communication

H. Jöstlein, Mechanism for the Rise in PSD . . . .", 6/89, unpublished

A 5m section of 1.5" dia. beam tube was cooled to liquid helium temperature and exposed to synchrotron radiation of up to 1 W/m in 10 mrad incidence. The synchrotron radiation spectrum (C.E.=300 eV) was closely matched to that of the SSC. A pair of quadrupole mass spectrometers sampled the emitted neutrals through 3mm dia. holes in the beam tube wall.

Experimental Findings

By far the most readily desorbed neutrals are hydrogen molecules. CO molecules are a distant second. Fig. 5 shows a time spectrum of desorbed hydrogen molecules, obtained by pulsing the synchrotron light with a vacuum disc chopper 120 times a second. Note that there is a clear desorption signal. The time response, although consistent with molecules of about 70K temperature, is actually a consequence of multiple bouncing in the beam tube and in the quadrupole enclosure.

A New Effect: Rise with Accumulated Dose

Data such as shown in Fig. 5 can be analysed in terms of hydrogen instantaneous density in the cold tube, hence beam lifetime in the Supercollider. Before doing so, however, we must deal with an unexpected observation. Fig. 6 shows the desorption rate for hydrogen molecules as a function of photon dose. A large increase, apparently linear with dose, is seen over the 12 hours of observation. To put the result into more familiar units, the hydrogen density is seen to increase about ten-fold, from an initial value of about $5\ 10^{-11}$ Torr (quoted as room temperature equivalent pressure, and measured at the quadrupole analyzer) to $1\ 10^{-9}$ Torr. The observation time was limited by the capacity of the helium dewar (1000 liters) available for these measurements.

When we changed the dewar, the beam tube warmed up to somewhere between 20K and 70K before cooling back down to 4.5 K. During that time the hydrogen pressure rose to 10^{-6} Torr, and some hydrogen escaped the beam tube. (Calculations show, however, that the bulk of H2 did not emerge from the beam tube due to the geometry and low velocity of the molecules).

---

[4] H. Ishimaru et al., The Journal of Accelerator Science and Technology, Vol. 2, No. 2, 79

On subsequent exposure to synchrotron radiation, a linear increase in hydrogen desorption is again seen, but at a lesser slope. After the next dewar change, the slope is seen to be even smaller.

Two Cold Desorption Mechanisms

These observations, together with more studies described below, lead to a description of cold desorption as a two-stage process.

The primary energetic photon, usually from synchrotron radiation, is thought to create an energetic electron through the photoelectric effect at the wall. This electron knocks an adsorbed molecule off the wall. The molecule leaves the wall with an energy appropriate to outer shell binding energies, a few eV or less. This is the same process that occurs in warm beam tubes. In a warm chamber, the molecule will eventually be removed by pumps. The pressure in the chamber results from the balance of newly desorbed molecules versus those removed by pumping.

The primary events leading to cold PSD are thought to be the same as those for warm PSD. But both the BNL and KEK experiments show an instantaneous density which is about an order of magnitude larger than that expected from the warm primary process, or measured from the primary cold process. This can be understood if the primary desorbed hydrogen molecule thermalizes during a few (perhaps 10) scatterings in the cold beam tube, losing in each scatter a fraction (half) of its initial energy. The resulting total time in flight is increased due to the extra crossings, and the instantaneous density is further increased due to the slower velocity of the molecules. This can account reasonably for the observed stronger signal, without inventing new mechanisms for cold desorption.

The cold desorption rate rises linearly with the accumulated photon dose, as explained above. This is in stark contrast to the drop of warm PSD with dose. In the same way that the warm PSD drops with dose because of a depletion of hydrogen on the surface, the cold PSD rate increases with dose because of an accumulation of previously desorbed hydrogen on the surface. We discussed above the way these hydrogen molecules thermalize (to 5K = 1 meV) during their scattering following the primary desorption. When they have become slow enough they will attach themselves to the wall with a probable binding energy a little above the thermal energy. This is analogous to adsorption at room temperature, where the most likely binding energy is a little higher than the thermal energy.

This process leaves an ever denser layer of very loosely bound hydrogen molecules on the wall surface. The presence of this loosely bound hydrogen is the chief change of the surface as the photon dose accumulates, and can explain the increased desorption with dose. The most likely agents are subsequently desorbed hydrogen molecules themselves. Each primary desorption event creates a hydrogen molecule of about 1 eV energy, many times larger than the binding energy (1 meV) of the loose hydrogen on the wall. Being of equal mass, the hydrogen molecule is likely to transfer a good fraction of its kinetic energy to the target molecule. Furthermore, when the dose reaches $5\ 10^{20}$ photons/m then the wall coverage is of order of a half monolayer. The probability of hitting another hydrogen molecule is then near certainty. The struck molecule will often have enough energy to release others from the wall, creating an avalanche of low energy hydrogen molecules. One could call this process "ballistic desorption".

The initial hydrogen molecule will take on order of 10 scattering events to reach 1 meV. In each of the scatterings, a new hydrogen molecule can be shaken loose, explaining the tenfold rise with dose. Ballistic desorption amplifies the number of slow molecules in flight, as the dose increases. Partial warmup of the cryostat drives the loosely bound molecules from the walls, either into pumps or onto more strongly binding sites.

Cleanup/pumping

A large cryogenic system such as the SSC cannot be quickly warmed sufficiently to pump the released hydrogen from the system. It is, however, relatively easy to raise the temperature to 20K or 30K. Hydrogen released at this temperature can migrate to the ends of the 17m dipole magnets, where one can think of intercepting it with pumps. These pumps might be in the form of a surface coating on the inside of the interface bellows assembly. Care must be taken and experiments need to be done to ensure that subsequently synchrotron light cannot redesorb the hydrogen, or heat the coatings sufficiently to cause thermal desorption. Rf heating by the pulsed beams must also be avoided. A perforated metal shield may help on both accounts. It may also be necessary to incorporate small heating elements to clean the coatings during warm pumping.

Beam Lifetime

Based on the above data, without cleanup, there will be a beam lifetime in excess of 150 hours, limited chiefly by proton loss due to nuclear scattering. Cleanup will extend this limitation considerably. Note, however, that beams will be replaced once a day in any case due to the unavoidable beam loss in the crossing points, and emittance growth due to a number of factors.

Leak Checking

The main rings will each have 3840 dipoles, 680 quadrupoles, and many lesser insertion devices. There will be a double wall beam tube connection, three helium and a liquid nitrogen connections (Fig. 7). All cold connections will be made by automated welding, requiring in excess of 50000 welds. The outer insulating vacuum sleeve is O-ring sealed (Fig. 8).

All internal connections must be leak tight, and are not accessible when cold. The helium connections pose the strictest requirements, expressed as a leak rate limit of 10-11 Torr l/s at room temperature.

Method to Find Internal Leaks

As with the Fermilab Tevatron, leaks will be detected by pressurizing the helium/nitrogen piping, and analyzing the helium contamination in the insulating vacuum space. One leak detector is required for each magnet interface, with all leak detectors sending data to a central unit.

The beam pipe connection is especially critical, since it is surrounded by liquid helium. To enable leak checking of the bellows assemblies they are double bellows units, with an annular vacuum space separating the beam tube vacuum from the helium space,. A thin sample tube goes to the outside for leak detection.

Leak Checking Equipment

Rather than using conventional special purpose leak detectors, the current thinking is to have pump carts with roughing/turbo pump combinations (see e.g. Fig. 9). These carts would be fitted with helium detection heads and controllers when used for leak detection. The carts would plug into a data bus in the tunnel for data transfer analysis. The turbo controllers should allow operation at a lower speed to reduce the compression ratio for helium, while maintaining full speed for water vapor, the main background gas.

Vacuum Operations

All vacuum systems will be pumped down initially using mobile turbo pump carts. These carts will maintain the insulating vacuum at about 10^{-4} Torr until cooldown, when the pressure will drop below 10^{-6} Torr. The many layers of thermal insulation will outgas at a large rate for long times, and it will be useful to use turbopumps that can produce useful compression at inlet pressures of a Torr or even higher, to bridge the gap in througput that exists in most roughing/turbo pump combinations.

Normally all carts will be removed after cooldown starts and the pressure becomes very low. If a helium leak, e.g. a cold leak, opens into the insulating vacuum then carts will be left connected near the leak site continuously. The data bus in the tunnel has provisions for readout and control of the carts.

The cold beam tube will be turbo pumped (through cold traps) to 10^{-5} Torr, when the ion pumps (one every 50m for a total of 792) are started. The pressure will not improve much until cooldown starts.

The ion pumps act also as pressure monitors during operation. The sensitivity of the total current readout of ion pumps is not very good, however. The challenge is to design a low cost helium monitor, sensitive well below 10^{-10} Torr. Such a monitor would greatly contribute to early leak detection and machine reliability, and would almost certainly be used in substantial numbers. Pirani type gauges will cover the high pressure range.

Cold Beam Valves

The proposed SSC will have 192 beam valves to partition the beam vacuum system. While the current design report conservatively assumed them to be installed in warm breaks, cold beam valves would be easier to fit, and could be deployed in larger numbers.

The purpose of the beam valves is

- to partition the system during construction

- to isolate leaking sections from the rest of the system

- to allow magnet replacement with only a local warm-up of the magnet string.

Cold Valve Properties:

1. Remote and automatic operation

2. Rf bridging across the valve when open to avoid heating the 5 K system by beam image currents. This requirement is less stringent than at electron machines due to the longer bunches at the SSC (6 cm), and may be satisfied by an Rf bridge around a fraction of the periphery. Detailed calculations need to be made for each design.

3. High Reliability. This includes very reliable status indication (remote and local; two independent devices?), simplicity of design in the cold parts, field replaceability of most components without warming up or breaking vacuum, repairability without cutting the valve out of the piping.

4. Open or stay-in-present-state under loss of power, control, gas pressure (yet to be decided).

5. Relatively fast closure (1 sec or less)

6. Lifetime of about 1000 closures

7. Very low heat input of 50 mW or less into the 5 K system

8. Short insertion length

9. Low cost (note that this item appears last in my list).

Vacuum Requirements of an SSC Cold Beam Valve

The SSC beam tube is of very small diameter (3 to 4 cm I.D.) and great length, with a large distance between rough pumping stations, perhaps 500m or more. In order to be able to rough pump the beam tube in a reasonable time with a minimum number of pump stations, it is necessary to have a clean beam tube which does not store large quantities of water and other gases on its surface. This means that oil films, porous oxide layers, and dust are to be avoided.

Beam valves should therefore be treated according to established UHV procedures. This includes degreasing and white-glove handling. No oil contamination is allowed, because oil might be carried into the beam tubes, and make pumpdown difficult.

Outgassing into the surrounding space is less critical. The valves are surrounded by insulating vacuum space. This space contains much organic material, is cryopumped, and requires a pressure of 10^{-6} to 10^{-7} Torr. No special requirements on the beam valves result, except that actuators, if located in the insulating vacuum must be reliably sealed and easily accessible for repair. It is desirable to place actuators outside the magnets for reliability and repairability.

Emergency Cold Closure - - Leak Rate Requirements

In a catastrophic magnet failure, the stored electric energy can burn a hole from the helium space through to the beam space. When the pressure wave in the beam space is detected, several partitioning valves to either side of the high pressure area will be automatically closed.

The amount of helium that is allowed to pass from one section into the next can be estimated under the assumptions that the section under vacuum should stay clean enough to allow helium leak checking within two days after warmup following the failure.If a leak-up to 1 Torr helium pressure is allowed, we can estimate the allowable leak rate for a single valve as 10^{-4} Torr l/sec as read on a leak detector.

A second requirement is that the amount of helium penetrating *two consecutive* beam valves must amount to less than 10^{-3} monolayers on the wall of the section beyond the second valve. This amount of helium is in equilibrium (at 5K) with a room temperature equivalent pressure of 10^{-10} Torr. This requirement leads to almost the same leak size requirement of the valve, about 10^{-4} at cc/s as measured on a standard leak detector.

It should be understood, however, that these numbers represent the worst case acceptable toward the end of the valve's life, and that valves with substantially lower leak rates will be preferred. The calculations are meant to show that for the cold beam valves reliability is more important than perfect sealing capability.

Valves requiring differential pumping can be used if they meet the above leak rate limits. Differential pumping would be only available one day after a failure event. Hybrid valve designs with an imperfect metal seal, backed by a cold tolerant elastomeric seal, can also be considered.

Electronics, Readout/Control

The SSC is so large that all readout and control functions must be available at a central control room. Communication will be achieved via a computer bus running along the tunnel. Electronic equipment will be located in wall recesses to avoid radiation damage. Table I shows data obtained at the Tevatron, and listed in the SSC Design Report. All devices such as HV power supplies, air cylinders etc. must conform to radiation hardness requirements, to be published by the SSC project management.

All devices must be operated from those crates, which will contain local processors. Local readout will be through plug-in portable computers.

Conclusions

The SSC provides a challenge to industry in many fields. Much work needs to be done in cooperation with the SSC laboratory to fill the new requirements and to come up with innovative products. We will all gain from this experience.

Figure Captions

Fig. 1 SSC Collider ring layout. The cluster regions provide space for experiments. The injector complex is shown near the west cluster. There are 10 refrigeration and power units around the ring (black diamonds).

Fig. 2 Tracks from an interaction at the Fermilab Tevatron. The tracks were measured with the CDF electronic detector, and reconstructed by computer. Many particles are created in each interaction.

Fig. 3 The injector system to the Supercollider. Starting with a source injecting protons into the Linac, the energy is raised by three successive booster synchrotrons to the 2 TeV injection energy (the 1986 design report, this picture, still suggests a 1 TeV injection energy).

Fig. 4 Thermal conductivity vs. pressure for the insulation package used in SSC dipoles.

Fig. 5 Time resolved proton desorption signal due to chopped synchrotron light. The time slot shown is roughly 10 msec. The slow turn-on is mostly due to hydrogen scattering in the beam tube and quadrupole enclosures.

Fig. 6 The Hydrogen desorption signal as a function of photon dose for three successive runs, with warmup to 20 to 70K in between. Note the strong increase with accumulated dose, and the slope reduction on successive runs.

Fig. 7 Isometric cutaway perspective drawing of the 6.6 Tesla SSC dipole magnet, showing all interconnect pipes.

Fig. 8 Longitudinal sections of the magnet interface piping. All connections are to be welded using automated equipment.

Fig. 9 Sketch of a pump cart, consisting of a roughing pump, turbo pump, cold trap and a gate valve with associated gauging, controls and computer interface. Such carts will be used for initial pumpdown, leak checking and leak pressure containment.

Table I **Summary of radiation measurements at 800 GeV in a typical tunnel section at Fermilab. Radiation hardness specification will be issued based on such measurements.**

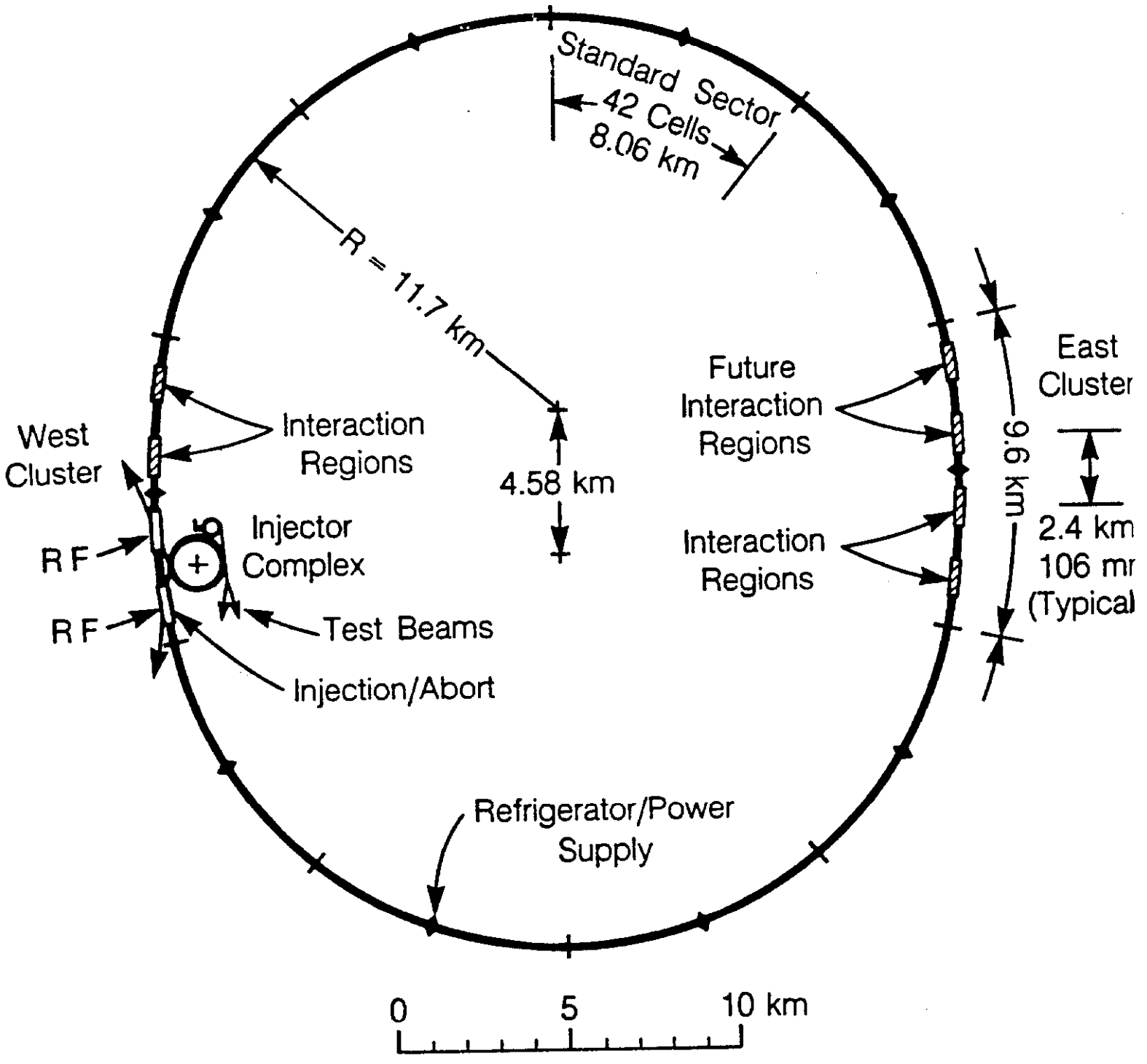

Fig. 1 SSC Collider ring layout. The cluster regions provide space for experiments. The injector complex is shown near the west cluster. There are 10 refrigeration and power units around the ring (black diamonds).

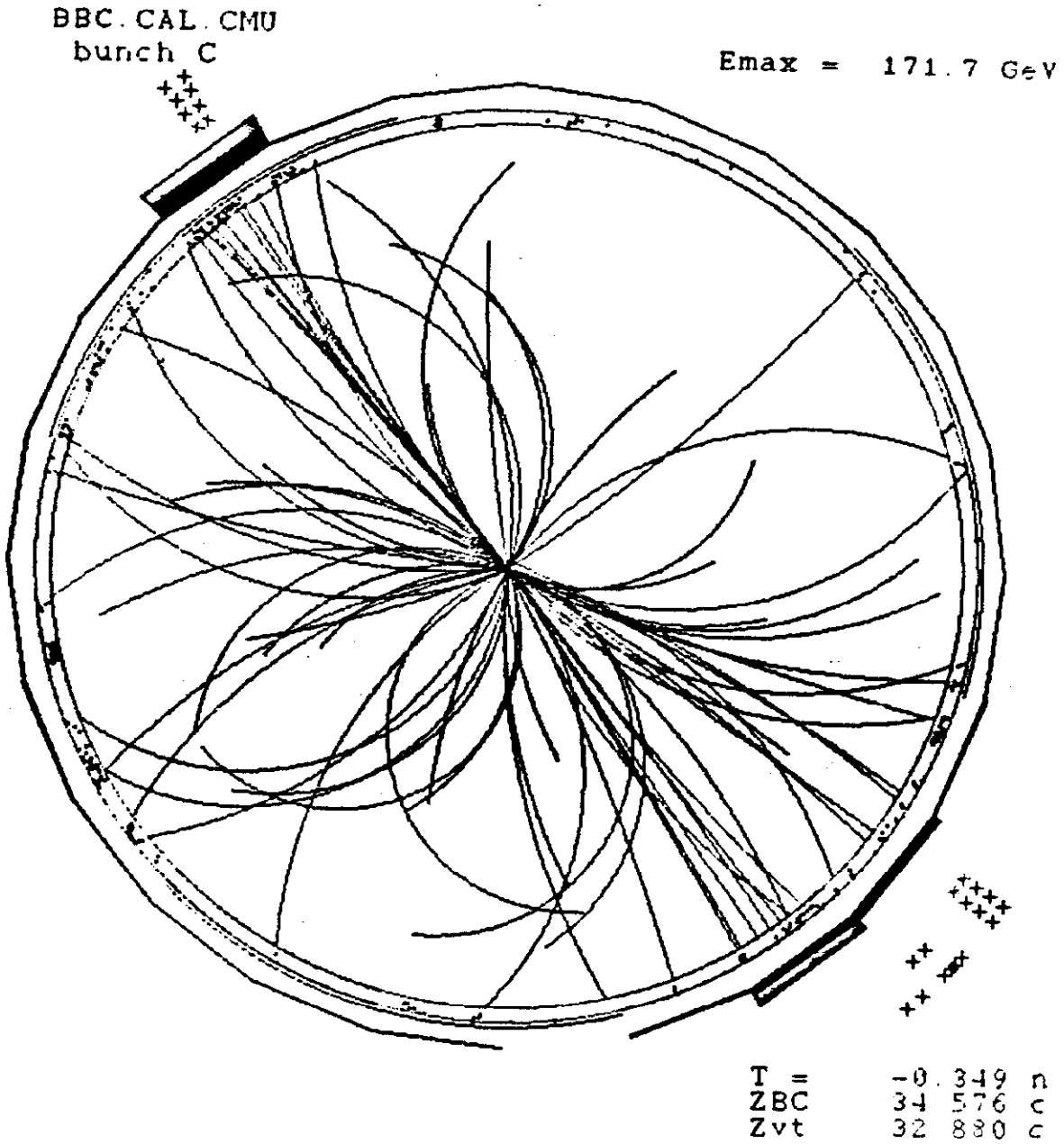

Fig. 2 Tracks from an interaction at the Fermilab Tevatron. The tracks were measured with the CDF electronic detector, and reconstructed by computer. Many particles are created in each interaction.

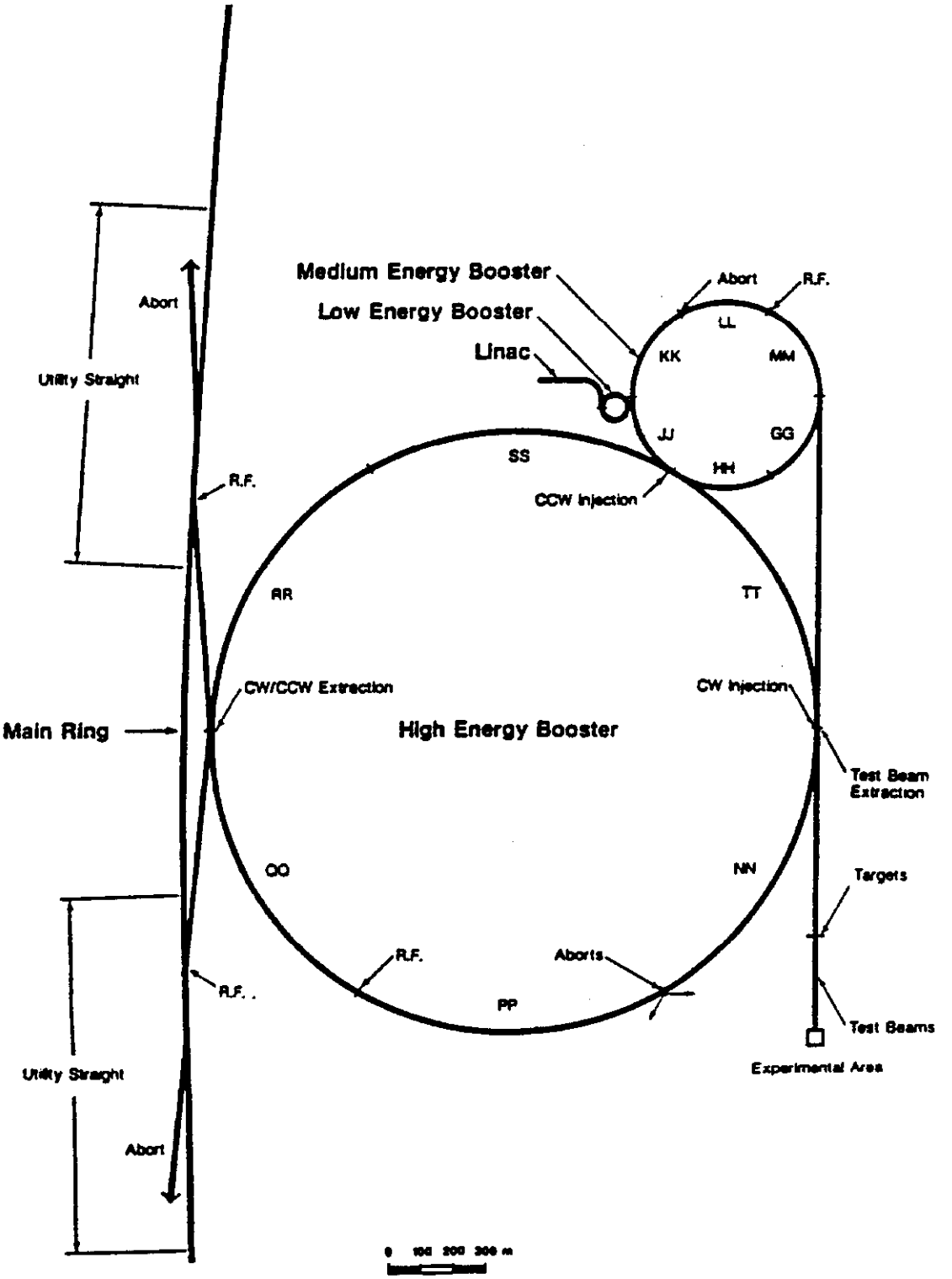

Fig. 3 The injector system to the Supercollider. Starting with a source injecting protons into the Linac, the energy is raised by three successive booster synchrotrons to the 2 TeV injection energy (the 1986 design report, this picture, still suggests a 1 TeV injection energy).

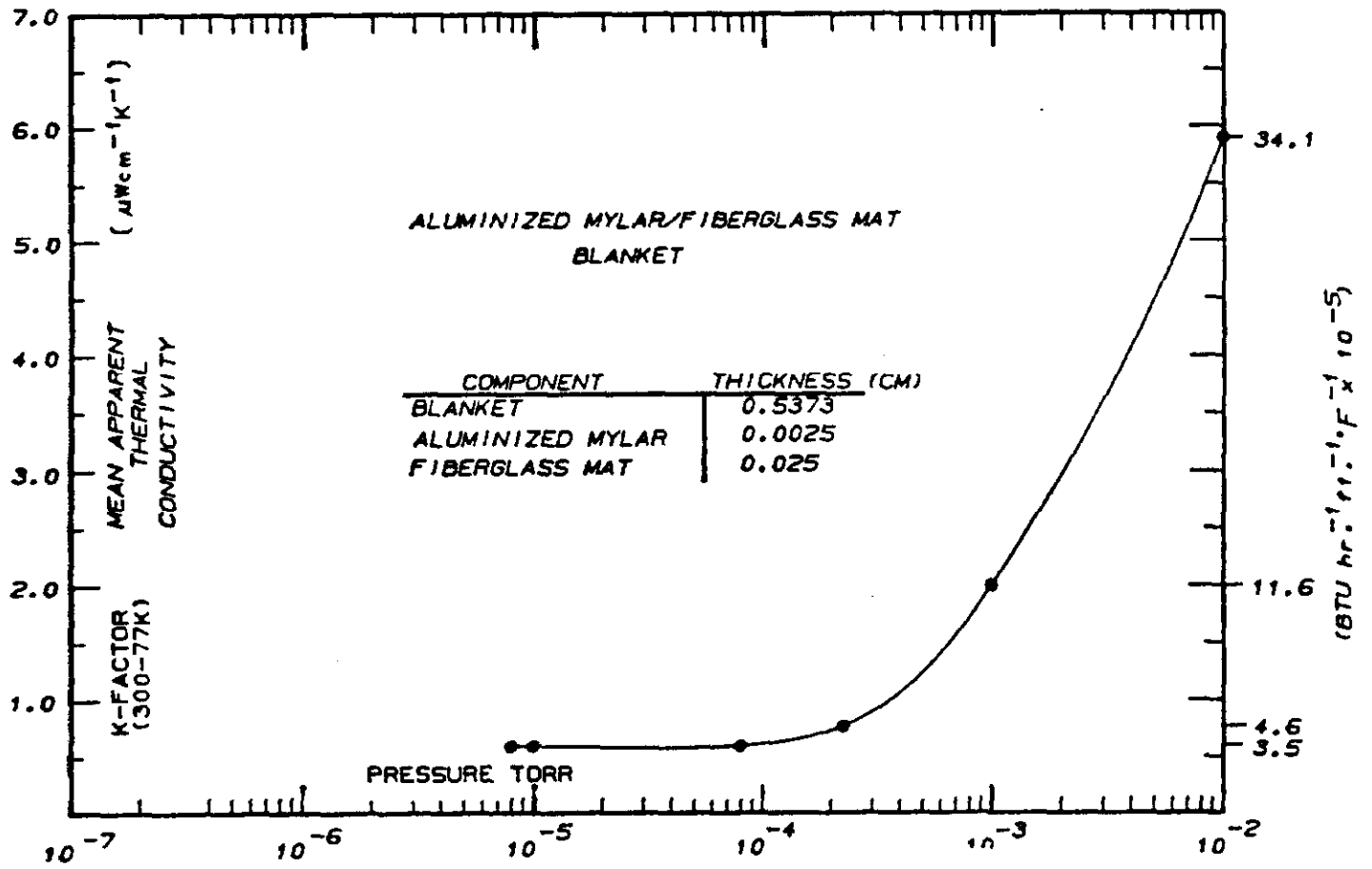

Fig. 4 Thermal conductivity vs. pressure for the insulation package used in SSC dipoles.

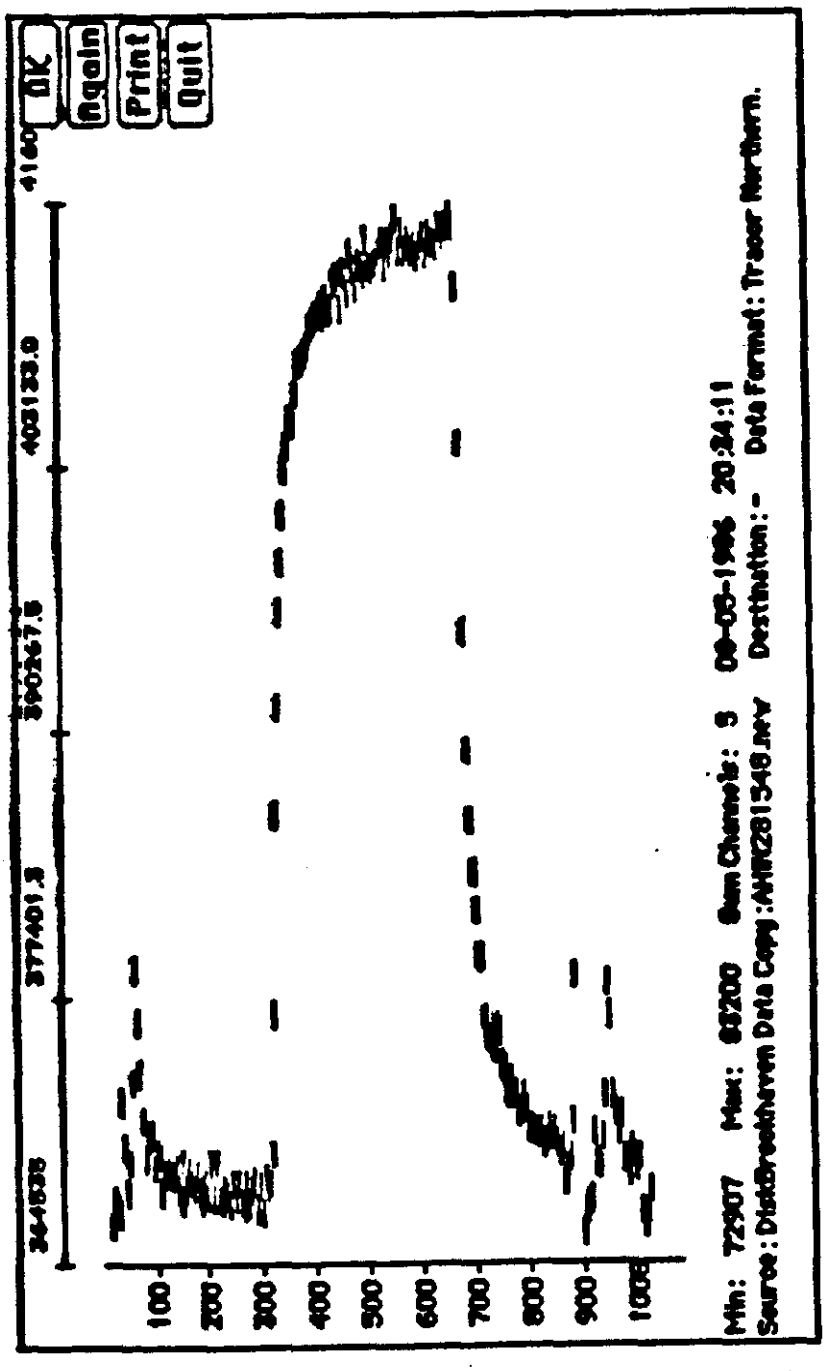

Fig. 5 Time resolved proton desorption signal due to chopped synchrotron light. The time slot shown is roughly 10 msec. The slow turn-on is mostly due to hydrogen scattering in the beam tube and quadrupole enclosures.

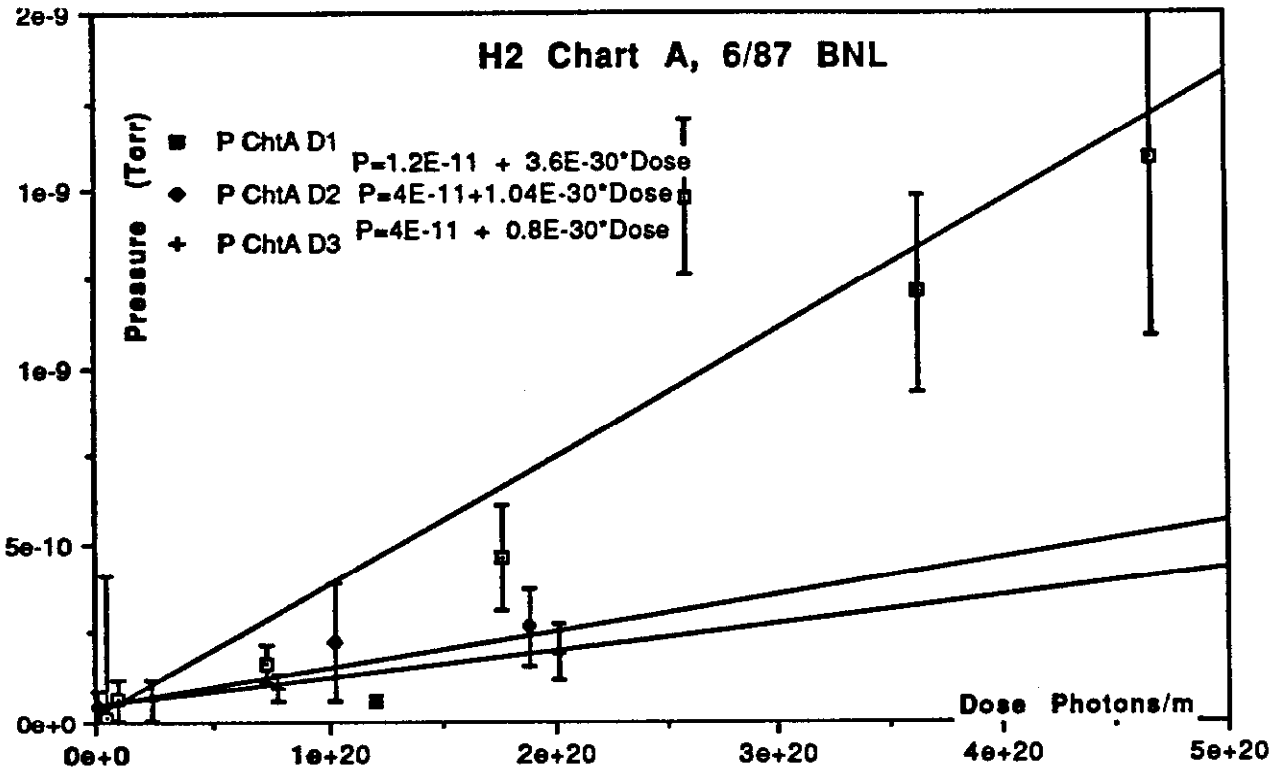

Fig. 6 The Hydrogen desorption signal as a function of photon dose for three successive runs, with warmup to 20 to 70K in between. Note the strong increase with accumulated dose, and the slope reduction on successive runs.

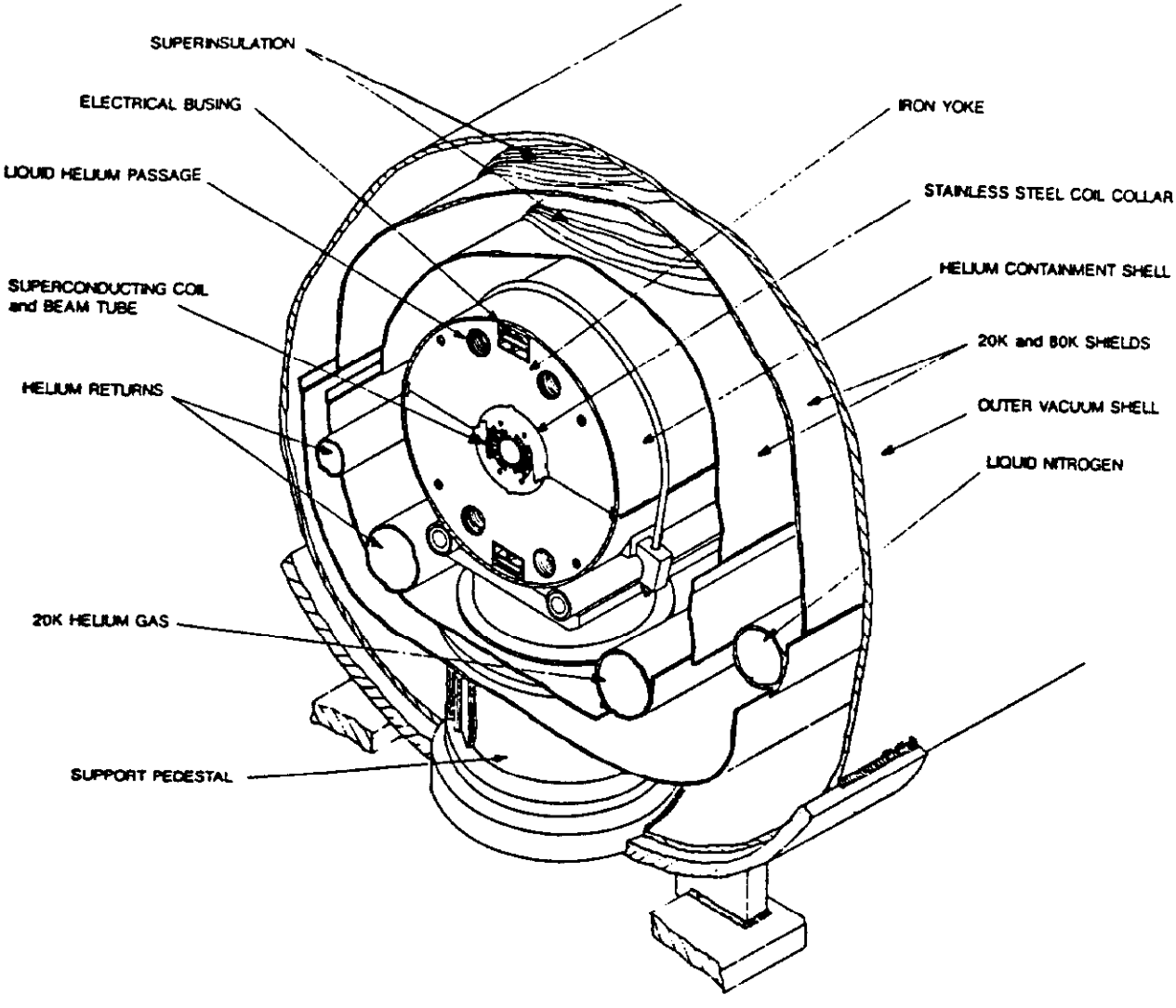

Fig. 7 Isometric cutaway perspective drawing of the 6.6 Tesla SSC dipole magnet, showing all interconnect pipes.

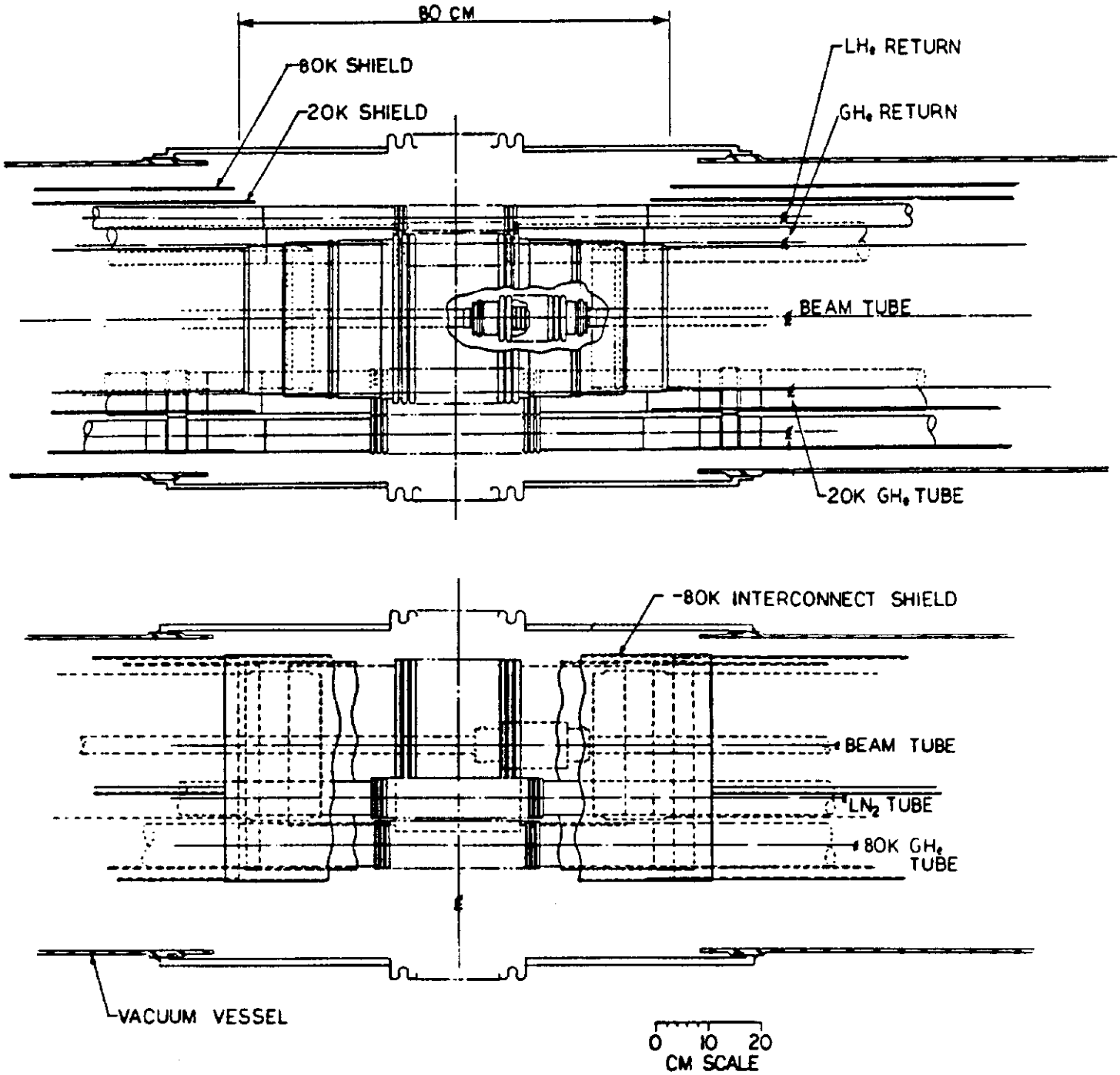

Fig. 8 Longitudinal sections of the magnet interface piping. All connections are to be welded using automated equipment.

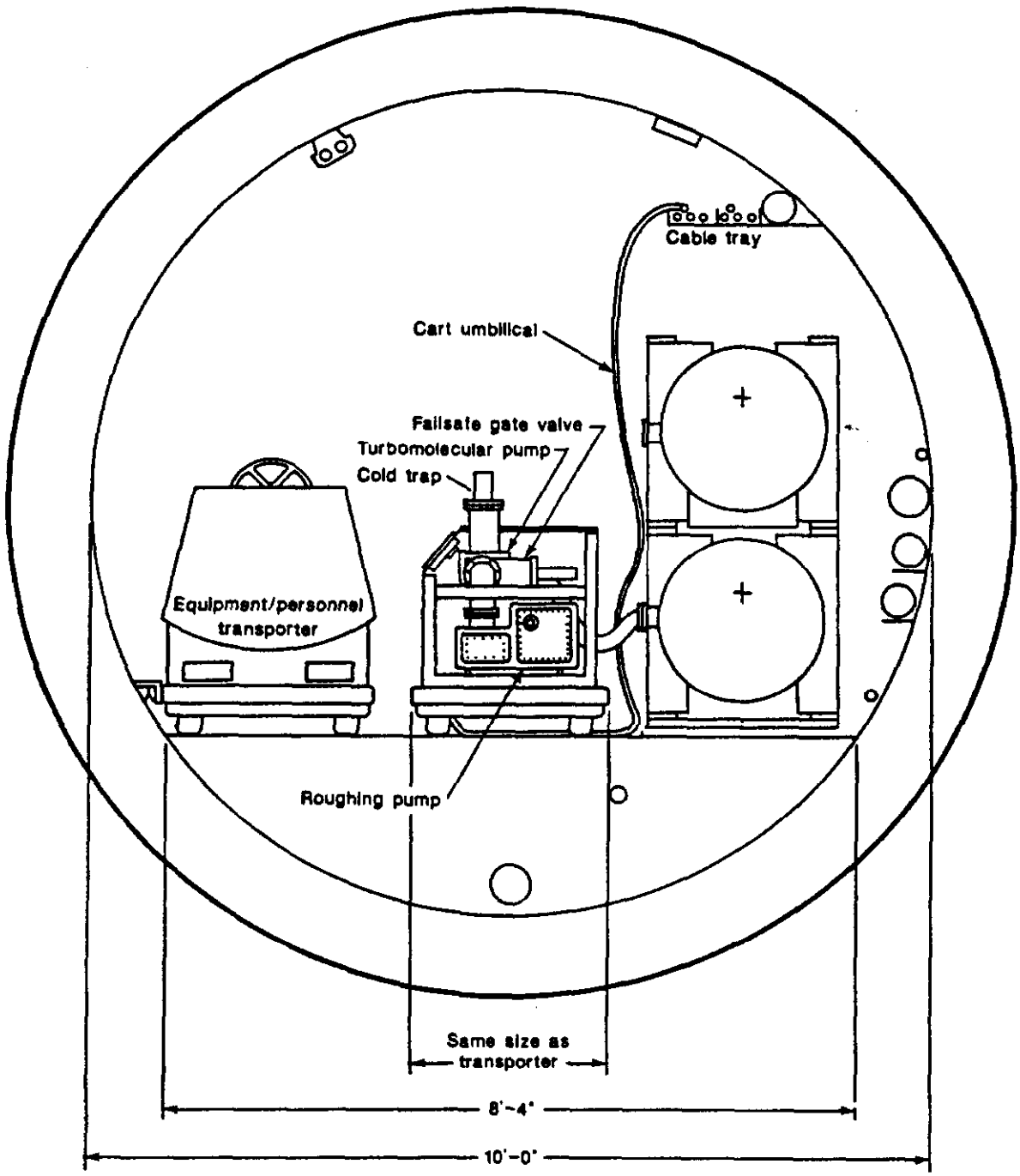

Fig. 9 Sketch of a pump cart, consisting of a roughing pump, turbo pump, cold trap and a gate valve with associated gauging, controls and computer interface. Such carts will be used for initial pumpdown, leak checking and leak pressure containment.

Summary of Radiation Measurements at 800 GeV [4.8-16]

Neutron flux @ 2.0 m	3.6 $cm^{-2}s^{-1}/10^{11}$ protons
Photon dose/neutron fluence	$<2\times10^{-11}$ Gy cm^2
Minimum ionizing dose/neutron fluence	$<2\times10^{-12}$ Gy cm^2
Fraction of neutrons with E > 1 eV	0.75
Fraction of neutrons with E > 1 keV	0.65
Peak in $Ed\phi/dE$ distribution	100 keV–1 MeV

Table I **Summary of radiation measurements at 800 GeV in a typical tunnel section at Fermilab. Radiation hardness specification will be issued based on such measurements.**